ISBN: 978-3-95450-231-8 ISSN: 2673-5490 doi: 10.18429/JACoW-IPAC2023-WEPA134

# DESIGN, FABRICATION AND MECHANICAL TESTS OF TIG-WELDED KA-BAND ACCELERATING STRUCTURES FOR ULTRA-HIGH GRADIENT APPLICATIONS

L. Faillace†, B. Spataro, INFN Laboratori Nazionali di Frascati, Frascati, Italy
M. Carillo, L. Giuliano, M. Migliorati, A. Mostacci, L. Palumbo, Sapienza University, Rome, Italy
V. Dolgashev, SLAC National Accelerator Laboratory, Menlo Park, USA
R. Bonifazi, Comeb srl, Rome, Italy



*Abstract*

The investigation of the processes, materials, technology and welding procedures used to manufacture accelerating components for maximum accelerating gradient (>100 MV/m) and minimum RF breakdown probability has led us to the proposal of hard-copper structures in Ka-Band made of multiple parts.

In this paper, we illustrate the TIG welding tests, including visual inspection and temperature monitoring, of Ka-band metallic RF cavities for the cases of two-half and four-quadrant models.

The RF cavities made of multiple parts operate at ultra-high accelerating gradients (well above >100 MV/m). Therefore, the following aspects of the welding procedure were used as references for the positive outcome of the process: 1) Successful execution of each weld bead/seam in order to assure vacuum tightness of the cavity. 2) The cleanliness of the inside surfaces of the cavities: visual inspection for absence of oxidation after cutting the cavity samples; 3) The temperature of the cavity surfaces always below the annealing one (mechanical properties significantly change after heating above 590 °C), in order to keep the hardness of the copper.

## INTRODUCTION

Operation at higher RF frequency permits the achievement of higher accelerating gradients. The first high power RF tests were conducted by Loew and Wang in 1984 and lead to an experimental curve of the breakdown events obviously correlated to the RF frequency.

Thanks to the technological improvements, a worldwide collaboration among SLAC, KEK, CERN and INFN was started more than two decades ago for the systematic high-gradient experiments of metallic RF accelerating structures.

Recently, braze-free cavities manufacturing, which does not involve any high-temperature processes, such as brazing and diffusion bonding, proved a noticeable increase in the achievable accelerating gradients with respect to heat-treated structures. Therefore, more experiments are foreseen. Moreover, proper material choice as well as mechanical and thermal treatments increase the maximum allowed field gradients and reduce the vacuum RF breakdown rate. From SLAC high-gradient tests, TIG and EBW welded hard-copper X-band RF cavities, from INFN-LNF [1-4].

For all the reasons above, we have come to list an example of a recipe that can produce viable ultra-compact and ultra-high gradient accelerating RF structures for certain applications (discussed in the following section):

- Frequency scaling to Ka-band (34-36 GHz);
- Adopting Open RF structures: "split-open" cavities made of two-halves, four quadrants or multiple-sectors;
- Hard-copper RF structures: material processing/handling below temperatures (about 800 - 1000 °C) that significantly change the mechanical properties → stay below Annealing (500 °C)→ TIG Welding.

As a consequence, a new project was recently proposed, the MICRON experiment, that was funded in 2022 by the INFN National Committee V. For this project, we will apply all our acquired experience from another previously funded experiment by the INFN Committee V, i.e. the Di-Electric and METallic Radiofrequency Accelerator (DEMETRA) experiment in 2015-2018.

## APPLICATIONS

The main applications of compact ultra-high gradient Ka-band RF accelerating structures are summarized in the following: research on RF Breakdown Rate and RF Breakdown Physics; electron beam longitudinal phase-space manipulation [5-11] in FELs (EuPRAXIA@INFN-LNF, CompactLight FEL, UC-XEL@UCLA); multi-frequency accelerators (S. Tantawi, SLAC); development of single and multi-frequency high-power RF klystrons [12-15].

## RF DESIGN

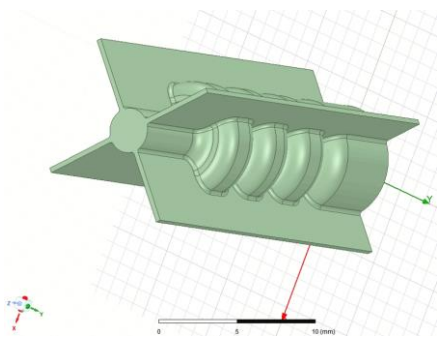

Figure 1: Four-quadrant Ka-band RF cavity.

† luigi.faillace@lnf.infn.it

ISBN: 978-3-95450-231-8 ISSN: 2673-5490 doi: 10.18429/JACoW-IPAC2023-WEPA134

The RF design was carried out with HFSS. We chose to use a three-cell cavity geometry [1, 2]. In these cavities, only the central cell's electric and magnetic fields mimic the fields of a periodic full-scale standing-wave structure. We refer to these types of cavities as "single cell" because the field is highest only in the middle cell, while the first and third cells have lower fields. The peak on-axis electric field in the middle cell is two times higher than in the end-cells for the purpose of localizing rf breakdowns mostly in the middle cell. This geometry was developed specifically to test the basic physics of rf breakdowns.

Due to the symmetry of the four-quadrant cavity, only one-eighth of the whole geometry was simulated. In Fig. 1, we show the electric field distribution on a symmetry plane. The corresponding on-axis filed profile is given in Fig. 2. The field is normalized to an accelerating gradient of 150 MV/m. The main RF parameters are listed in Table 1.

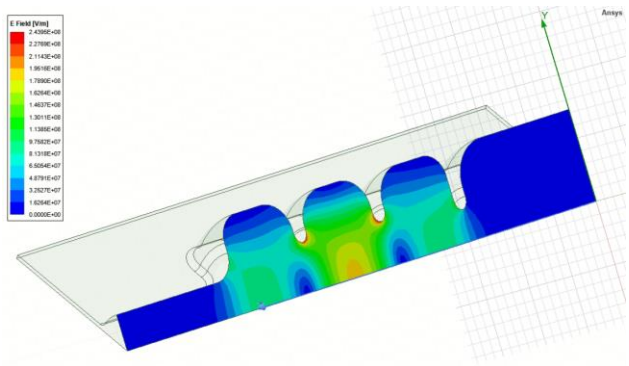

Figure 1: Electric field distribution on symmetry plane. One-eighth of the whole structure is simulated with HFSS. The field is normalized to an accelerating gradient of 150 MV/m.

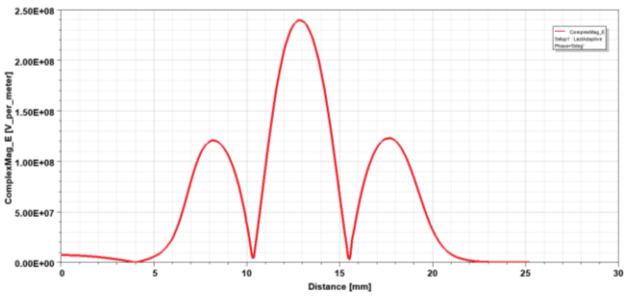


Figure 2: On-axis electric field profile. The field is normalized to an accelerating gradient of 150 MV/m.

From our design, there are some crucial aspects which highlight the advantages of using an RF cavity made of four sectors with respect to the same cavity geometry but with no sectors:

- Similar longitudinal shunt impedances;
- Higher lower-modes separation;
- Higher vacuum pumping capacity through the cuts;
- The quality factor decreases by only 2%.

Moreover, the advantage of performing the TIG welding on the outer slots which avoids high temperature brazing and/or diffusion bonding processes (the typical assembly methods widely used to manufacture ultrahigh vacuum accelerating devices) which - occurring at about 800–1000 °C - significantly change the cavity mechanical properties.

Table 1: Main RF Parameters

| Parameter | Value |
|---|---|
| Resonant frequency, f [GHz] | 35.982 |
| Quality factor Q | 6000 |
| Shunt impedance [MΩ/m] | 160 |
| Hmax [MA/m] | 0.6 |
| Emax [MV/m] | 400 |
| Power loss [MW] | 0.75 |
| a [mm] | 2 |
| a/λ | 0.24 |
| t [mm] | 0.635 |
| Iris ellipticity | 1.38 |
| Accelerating Gradient (MV/m) | 150 |
| Phase advance per cell (deg) | 180 |

## MANUFACTURING OF SAMPLES

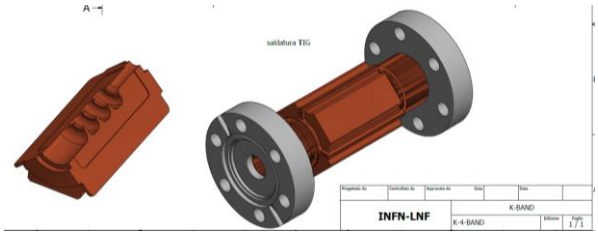


Figure 3: Drawing of the 4-quadrant structure prototype for TIG welding.

The drawing of the 4-quadrant structure prototype for TIG welding and morphological tests is shown in Fig. 3. All cavity sectors were manufactured by using a CNC 5-axis milling machine at Comeb and are shown in Fig. 4. The choice of the machining tool (mono/poly-crystalline diamond) is crucial, depending on the required tolerance and roughness:

- Tungsten-carbide tool → Tolerance = +- 10 µm; Roughness with Ra = 1.6 µm.
- Diamond tool with spherical radius < 1 µm → Tolerance = +- 5 µm; Roughness with Ra < 80nm.

Figure 4: 4-quadrant structure samples before assembly and TIG welding.

ISBN: 978-3-95450-231-8 ISSN: 2673-5490 doi: 10.18429/JACoW-IPAC2023-WEPA134



## TIG WELDING TESTS

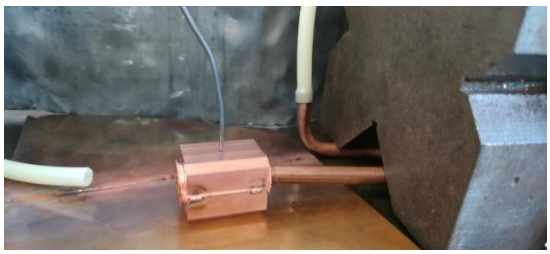

Figure 5: Experimental Set-up for TIG welding. Argon mixture is fused through cavity during welding.

Experimental Set-up for TIG welding of the samples is shown in Fig. 5 and described below:

- The TIG welding was performed with the use of protective gas from the torch (50% He, 50% Ar) with flow set at 13 l/min;
- Further flushing of inert gas was applied inside the cavities (100% Ar);
- The maximum current value set on the TIG machine was 175 A;
- A thermocouple was placed on the cavity inner surfaces through a hole in the cavity body;
- The data for the temperature plots were obtained from the video recordings.

We created a checkout list in order to judge upon the procedure outcome:

1. Successful execution of each weld bead/seam in order to assure vacuum tightness of the cavity.
2. The cleanliness of the inside surfaces of the cavities: visual inspection for absence of oxidation after cutting the cavity samples;
3. The temperature of the cavity surfaces always below the annealing one (mechanical properties significantly change after heating above 590 ˚C), in order to keep the hardness of the copper.


Figure 6: A picture of the cavity taken after the cleaning process to remove the external dirt on the outer surfaces due to the welding.

In Fig. 6, it is a picture of the cavity taken after the cleaning process to remove the external dirt on the outer surfaces due to the welding. For this bead the welding was performed at 125 A with a peak temperature of 252 °C, as shown in Fig. 7. The weld seam was observed to be well executed. We have to notice that a similar behavior applies to all samples that we welded: - satisfactorily welding of all teeth; - the temperature of the cavity quadrants always below copper annealing.

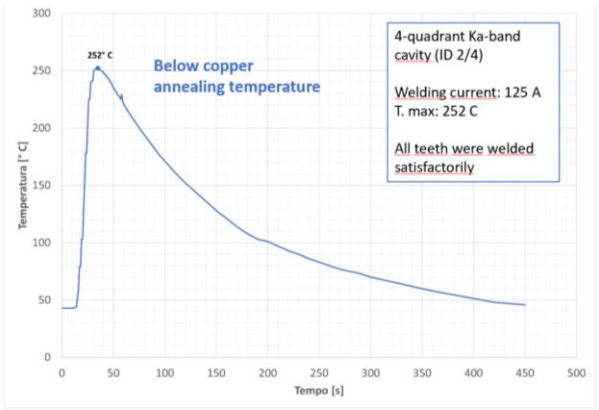


Figure 7: Recorded temperature distribution on cavity RF surfaces.

## CONCLUSIONS

We opened the four-quadrant cavity. This cavity (like the others) had been kept in a protective nitrogen atmosphere for the entire period since the welding process. The opening was carried out by removing one of the four weld seams by means of a Dremel cutter in order to avoid thermal alterations. The appearance of the cavity was shiny and there were no traces of oxidation in the areas where there was direct flushing of argon.

The central area where argon was flowing the appearance remains bright. At a visual analysis, there were traces of oxidation. The areas closest to the weld seam showed instead the presence of oxide, but it is to be considered that in those areas due to the direct contact between the surfaces to be welded, the presence of inert gas was absent and therefore such result was expected.

Particular attention will be addressed to fixtures that will be optimized for the alignment of the sectors.

By applying the same welding procedure and skill sets learned from the fabrication and welding of the first cavity samples made of multiple sectors described in this paper, the next goal in the MICRON project is to build a multi-cell cavity with mode launcher for low RF power tests.

## ACKNOWLEDGEMENTS

This work was supported by the INFN Committee V for the funding of the MICRON experiment.

## REFERENCES

[1] V. A. Dolgashev, L. Faillace, B. Spataro, and R. Bonifazi. "Innovative compact braze-free accelerating cavity." *Journal of Instrumentation* 13, no. 09 (2018): P09017.

[2] V. A. Dolgashev, L. Faillace, B. Spataro, S. Tantawi, and R. Bonifazi. "High-gradient rf tests of welded X-band accelerating cavities." *Physical Review Accelerators and Beams* 24, no. 8 (2021): 081002.

ISBN: 978-3-95450-231-8 ISSN: 2673-5490 doi: 10.18429/JACoW-IPAC2023-WEPA134

[3] L. Faillace, B. Spataro, M. Behtouei, M. Carillo, V. Dolgashev, G. Mauro, M. Migliorati, G. Torrisi, "Design and Prototyping of high gradient Ka-band accelerating structures", *International Workshop on Breakdown Science and High Gradient Technology (HG2022)*, poster presentation.

[4] V. A. Dolgashev, L. Faillace, Y. Higashi, A. Marcelli, B. Spataro, R. Bonifazi, "Materials and technological processes for High-Gradient accelerating structures: new results from mechanical tests of an innovative braze-free cavity", *Journal of Instrumentation*, 2020 Jan 27;15(01):P01029.

[5] M. Behtouei, L. Faillace, M. Migliorati, L. Palumbo, B. Spataro, "New Analytical derivation of Group Velocity in TW accelerating structures", in *Journal of Physics: Conference Series* 2019 Nov 1 (Vol. 1350, p. 012112). IOP Publishing.

[6] M. Behtouei, L. Faillace, B. Spataro, A. Variola, and M. Migliorati, "A SW Ka-band linearizer structure with minimum surface electric field for the compact light XLS project", *Nuclear Instruments and Methods in Physics Research Section A: Accelerators, Spectrometers, Detectors and Associated Equipment* 984 (2020): 164653.

[7] M. Behtouei, L. Faillace, B. Spataro, A. Variola, and M. Migliorati, "A novel exact analytical expression for the magnetic field of a solenoid", *Waves in Random and Complex Media* 32, no. 4 (2022): 1977-1991.

[8] B. Spataro, M. Behtouei, L. Faillace, A. Variola, V. A. Dolgashev, J. Rosenzweig, G. Torrisi, and M. Migliorati, "Ka-band linearizer for the Ultra-Compact X-ray free-electron laser at UCLA", *Nuclear Instruments and Methods in Physics Research Section A: Accelerators, Spectrometers, Detectors and Associated Equipment* 1013 (2021): 165643.

[9] A. Castilla, R. Apsimon, G. Burt, X. Wu, A. Latina, X. Liu, I. Syratchev, W. Wuensch, B. Spataro, A. W. Cross, "*Ka-band linearizer structure studies for a compact light source"*, Physical Review Accelerators and Beams. 2022 Nov 9;25(11):112001.

[10] A. Leggieri, M. Behtouei, G. Burt, F. Di Paolo, B. Spataro, "A novel harmonic klystron configuration for high power microwave frequency conversion", arXiv preprint arXiv:2212.12359. 2022 Dec 23.

[11] A. Castilla, L. Zhang, X. Wu, W. Wuensch, B. Spataro, A. Latina, A. W. Cross, G. Burt, I. Syratchev, M. Behtouei, X. Liu X, "Development of 36 GHz RF Systems for RF Linearisers", in *Proc. IPAC'21*, Online, 24 - 28 May 2021, pp.4518-4523.

[12] M. Behtouei, B. Spataro, F. Di Paolo, A. Leggieri, "The Ka-band High Power Amplifier Design Program of INFN", *Vacuum* 191 (2021) 110377.

[13] B. Spataro, M. Behtouei, F. Di Paolo, A. Leggieri, "A low-perveance electron gun for a high-efficiency Ka-band klystron", *The European Physical Journal Plus*. 2022 Jul 5;137(7):769.

[14] M. Bethouei, B. Spataro, L. Faillace, M. Carillo, A. Leggieri, L. Palumbo, and M. Migliorati, "Relativistic versus non-relativistic approaches to a low perveance high quality matched beam for a high efficiency Ka-band Klystron", *Instruments* 5, no. 4 (2021): 33.

[15] F. Marrese, L. Valletti, S. Fantauzzi, A. Leggieri, M. Behtouei, B. Spataro, and F. Di Paolo. "Multiphysics design of high-power microwave vacuum window", *Journal of Microwaves, Optoelectronics and Electromagnetic Applications* 21 (2022): 157-170.